Effects of novel mRNA-VEGF@USPIO nanoparticles on human brain microvascular endothelial cell injury

Jiang Zhao[1,2] and Zhiyuan Qian[1]

[1] *Department of Neurosurgery, The Second Affiliated Hospital of Soochow University, Suzhou, China*
[2] *Department of Neurosurgery, Shanghai Punan Hospital of Pudong New District, Punan Branch of Renji Hospital, Shanghai Jiaotong University School of Medicine, Shanghai, China*

Abstract. We investigated the effect of mRNA-VEGF@ultrasmall superparamagnetic iron oxide (USPIO) nanoparticles on the repair of human brain microvascular endothelial cell (HBMECs) injury and its related mechanisms. mRNA-VEGF@USPIO nanoparticles were designed, prepared, and characterized using NTA and UV spectrophotometry. Cell viability was determined using the CCK-8. Cells in the control, TNF-α, and mRNA-VEGF@USPIO groups were sequenced and the differentially expressed genes (DEGs) were identified. Finally, a functional analysis of the DEGs was performed. Both NTA and spectrophotometry results indicated that mRNA-VEGF@USPIO was successfully constructed. TNF-α significantly reduced cell viability and promoted apoptosis compared with the control group ($p < 0.05$), whereas mRNA-VEGF@USPIO nanoparticles reversed the changes caused by TNF-α. *Via* sequencing, 9063 DEGs were identified between the control and TNF-α groups, 9125 DEGs were identified between the control and mRNA-VEGF@USPIO groups, and 211 DEGs were identified between the TNF-α and mRNA-VEGF@USPIO groups. Additionally, 71 overlapping DEGs were identified in the three groups using Venn diagrams. These overlapping DEGs were mainly enriched in cytokine-cytokine receptor interactions and the TNF signaling pathway, NF-κB signaling pathway, and NOD-like receptor signaling pathway. This study shows that mRNA-VEGF@USPIO nanoparticles can repair HBMECs injury.

Key words: Ultrasmall superparamagnetic iron oxide — Human brain microvascular endothelial cells — Nanoparticles — Differentially expressed genes

Introduction

Human brain microvascular endothelial cells (HBMECs) are important tissue components for maintaining the blood-brain barrier and play a crucial role in maintaining the homeostasis of the cerebrovascular system (Katt et al. 2016; O'Connor et al. 2020). HBMECs not only serve as a barrier to maintain tissues and blood, but also play a role in a variety of biological functions. HBMEC injury can

contribute to the development of ischemic brain disease, and oxidative stress can exacerbate vascular endothelial cell injury. HBMEC injury and dysfunction can disrupt the blood-brain barrier, eventually leading to a variety of neurological diseases, such as cerebral edema, brain tumors, and cerebral ischemia (Göthe et al. 2012; Deng et al. 2020; Jiang et al. 2020). Therefore, it is important to research drugs that can repair endothelial cell damage in cerebral blood vessels.

Vascular endothelial-derived growth factor (VEGF) is a hypoxia-inducible protein with angiogenic and vascular permeability-enhancing properties (El-Sayed Mohammed Youssef et al. 2015). VEGF is a key regulator of endothelial cell function. Under critical conditions in neuronal cells (hypoxia, glucose deprivation, and oxidative stress), VEGF mediates multiple molecular responses, leading to the inhibition of programmed cell death and the stimulation of neurogenesis

(Ikeda et al. 2006; Ferrara 2009; Eichmann and Simons 2012). In addition, VEGF indirectly exerts neuroprotective effects through several mechanisms, such as stimulating angiogenesis, enhancing the permeability of the blood-brain barrier to glucose, and activating antioxidants (Candelario-Jalil 2009; Kim et al. 2021). Studies have shown that VEGF is regulated in a complex and coordinated manner during endothelial injury (Nag et al. 2002; Abadie et al. 2005; Catar et al. 2021). Therefore, VEGF may be an important regulator for the repair of brain microvascular endothelial cell injury.

Traditional means of drug delivery include ingestion orally or *via* injection; however, these methods have significant disadvantages, including increased pain and difficulty in targeting the disease area. Gene therapy can be used to treat certain diseases by introducing genetic material into cells (Kay et al. 2001; Mammen et al. 2007). Currently, gene therapy mainly involves viral and liposomal vectors; however, these therapies have certain limitations and shortcomings (Sun et al. 2014; Ediriweera et al. 2021). Therefore, small-nanoparticle vectors have been gathering interest. Ultrasmall superparamagnetic iron oxide (USPIO) has been used in an increasing number of studies because its inner core diameter is between 3–15 nm (Schütz et al. 2014; Richard et al. 2016). USPIO can be combined with specific factors, such as antibodies, proteins, and drugs to act on specific cells (Corot et al. 2006; Shakil et al. 2019). Therefore, in this study, we investigated the effects of mRNA-VEGF@USPIO nanoparticles, that is, endothelial cell probes, on injured endothelial cells. The nanoparticles were designed and prepared. Additionally, a high-throughput sequencing method was used to identify the crucial genes of the nanoparticles in endothelial injury repair and to identify the possible molecular mechanisms to provide a research basis for clinical treatment.

Methods

Preparation of USPIO

USPIO was prepared according to previously reported methods (Di Marco et al. 2007; Youwei Li et al. 2012; Rui et al. 2016). In this study, we prepared USPIO *via* three methods. First, 8 g sodium hydrate (NaOH) was dissolved in 80 ml Di (ethylene glycol) (DEG) through ultrasonic stirring and microwave heating (Solution B). Solution B was then kept in an oven at 72°C until use. Thereafter, 23.07 g of poly (acrylic acid) (PAA, 30%) and 7.8 g of $FeCl_3$ were dissolved in 360 ml DEG through microwave heating and ultrasonic stirring (Solution A). Solution A was then heated to 220°C by microwave under vigorous stirring, and the pre-heated Solution B (72°C) was added to Solution A. After constant heating for 10 min, the mixture was then cooled down to approximately 40°C and Fe_3O_4 colloids were obtained and then purified with a roll film small testing machine (JM1812-1, Jinan Bona Biotechnology

Co. LTD, Jinan, Shandong). The nanoparticles obtained were USPIO-1. Furthermore, a precipitation method was used to synthesize USPIO-2. Briefly, 3 mmol of PAA and 4 mmol of $FeCl_3$ were added to 30 ml of DEG, followed by 30 mmol of urea. After incubated at 200°C for 12 h, the mixture was cooled to room temperature, and then 90 ml ethyl alcohol was added. After 20 min of ultrasound stirring and 10 min of magnet adsorption, the sediments were resuspended in 160 ml ultrapure water and 160 μl NaOH (1 M), which yielded USPIO-2. In addition, positively modified USPIO-3 was obtained using a physical adsorption method.

Construction of mRNA-VEGF@USPIO probes

The VEGF mRNA was synthesized by Huzhou Hippo Bio Co. (Zhejiang, China). Briefly, approximately 40 μg of VEGF mRNA was dissolved in 0.1 ml polyethyleneimine (PEI) solution (10 mg/ml, #S24087, Shanghai Yuanye Bio-Technology Co., Ltd, Shanghai, China), and was then placed in a rotary reactor at 37°C for 1 h, which yielded PEI@mRNA-VEGF. Then, USPIO-3 (1 mg) was added to PEI@mRNA-VEGF and the mixture was incubated in a rotary reactor at 37°C for further 2 h. Thereafter, the mixture was centrifuged at 3000 rpm for 5 min and the supernatant (mRNA-VEGF@USPIO) was collected for further experiments.

Characterization of USPIO and mRNA-VEGF@USPIO probes

Different USPIO samples (USPIO-1, USPIO-2, and USPIO-3) were used for dynamic light scattering (DLS) measurements using a Zetasizer Nano (Malvern, UK) and transmission electron microscopy (TEM, Olympus). The constructed mRNA-VEGF@USPIO samples were also used to determine the particle size using a NanoSight nanoparticle size analyzer (NTA, Malvern), and the mRNA content was determined using Qubit.

Cell culture

HBMECs, purchased from Shanghai Zhong Qiao Xin Zhou Biotechnology Co., Ltd. (Shanghai, China), were cultured in M199 medium (CM-H124, Procell) supplemented with endothelial cell growth supplement and 10% fetal bovine saline (FBS) and maintained at 37°C with 5% CO_2. Cell passaging was performed when the cells reached 80–90% confluence.

Prussian blue dyeing and TEM observation

The HBMECs were seeded in 12-well plates at a density of 1×10^5 cells/well and cultured overnight. The next day, medium containing USPIO or mRNA-VEGF@USPIO was added, and the cells were cultured for further 12 h. After washing with PBS three times, the cells were fixed with 4% glutaraldehyde for 20 min, and then stained with Prussian blue dye (1 g potassium

ferrocyanide dissolved in 9 ml distilled water, and then mixed with 1 ml 36–38% hydrochloric acid) at 37°C for 30 min. After washing, the cells were re-stained with Nuclear Fast Red for 3 min and observed under an inverted microscope (Olympus).

The fixed cells were washed with PBS three times and were then fixed with 1% osmium tetroxide at 4°C for 3 h. After dehydration with different concentrations of ethanol (70% for 5 min, 95% for 10 min, and 100% for 10 min), the cells were embedded in Epon 812 and cut into 75 nm-thick slides. After staining with uranium acetate and lead citrate for 3 min, the slides were observed and photographed using TEM (Olympus).

Inductively Coupled Plasma Optical Emission Spectrometry (ICP-OES)

To verify the specific targeting of different types of USPIO nanomaterials to HBMECs, ICP-OES was used to detect the quantitative uptake ability of HBMECs by the three types of USPIO nanomaterials. Briefly, cells were seeded in a 24-well plate and cultured overnight. The next day, the medium was changed to one containing different amounts of USPIO and cultured for another 4 h. After centrifugation at 1000 rpm for 3 min, 0.2 ml aqua regia was added to the cells and cultured overnight. Thereafter, ICP-OES was conducted to analyze the iron (Fe) content in each sample.

Cell viability assay

Cell Counting Kit-8 (CCK-8) assays were used to study the viability of the cultured HBMECs. HBMECs were seeded at a density of 1×10^5 cells/well in 6-well plates and incubated overnight. The next day, tumor necrosis factor-α (TNF-α, 10 ng/ml) with/without mRNA-VEGF@USPIO nanoparticles (32 μg/ml) was co-cultured with HBMECs for 24 h, 48 h and 72 h. Thereafter, 10 μl of CCK8 reagent was added to each well and incubated for 2 h. Absorbance was recorded at 450 nm.

Transcriptome sequencing

The HBMECs were divided into three groups: HBMECs, HBMECs+TNF-α, and HBMECs+TNF-α+mRNA-VEGF@ USPIO groups. The cells in the HBMECs group were un-treated; the cells in the HBMECs+TNF-α group were cultured in medium containing 10 ng/ml TNF-α; and the cells in the HBMECs+TNF-α+mRNA-VEGF@USPIO group were maintained in medium supplemented with 10 ng/ml TNF-α and 32 μg/ml mRNA-VEGF@USPIO nanoparticles. After culturing for a further 48 h, HBMECs with different treatments were harvested to isolate total RNA using TRIzol (Invitrogen, Carlsbad, CA, USA), according to the manufacturer's instructions. mRNA was enriched from total RNA using oligo (dT) magnetic beads, fragmented, and reverse transcribed into double-stranded cDNA. Finally, the sequencing adapter was ligated into the fragments. All libraries were sequenced using the Illumina HiSeq system (Illumina Inc., San Diego, CA).

The raw sequences were first filtered by removing linker and low-quality sequences, including low-quality bases (quality value <30) at the end of the sequence (3' end), reads with an N ratio >10%, and adapters, and then quality trimmed to a length of <50 bp. RSEM software was used to calculate fragments per million mapped reads *per* kilobase transcript (FPKM) to elucidate gene expression. Differential gene expression analyses were performed using DESeq. The |log₂fold-change (FC)| ≥ 1 and the adjusted $p < 0.05$ were used as the threshold for significant differential expression. Annotation was based on the Clusters of Orthologous Genes, Gene Ontology (GO), and Kyoto Encyclopedia of Genes and Genomes (KEGG) databases.

Quantitative reverse transcription-polymerase chain reaction (qRT-PCR)

Total RNA was reverse-transcribed into cDNA using the PrimeScript™ RT Master Mix Kit (TAKARA, Japan), and qPCR procedures were carried out using the Power SYBR Green PCR Master Mix (Thermo Fisher). The relevant lncRNA expression levels were calculated using the $2^{-\Delta\Delta CT}$ method. *GAPDH* was used as the reference gene. Table 1 lists the primer sequences used in this study.

Table 1. Primer sequences

| Primer		Sequence (5′–3′)
GAPDH	F	TGACAACTTTGGTATCGTGGAAGG
	R	AGGCAGGGATGATGTTCTGGAGAG
TNF-α	F	GAGGCCAAGCCCTGGTATG
	R	CGGGCCGATTGATCTCAGC
VEGF	F	AGGGCAGAATCATCACGAAGT
	R	AGGGTCTCGATTGGATGGCA
PCDH1	F	ACGCCACTCGGGTAGTGTA
	R	TCACGGTCGATGGAGGTCTC
ABCG4	F	CCGTGGACATCGAGTTCGTG
	R	TGAGAGGCACTTGAGAAGGGT
SERPINA1	F	ATGCTGCCCAGAAGACAGATA
	R	CTGAAGGCGAACTCAGCCA
RIMS1	F	GCCGAGCCGAGAGTCTACT
	R	TCCACTTCTAATTGGCCCTTTTT
NDRG2	F	AGACTCACTCTGTGGAGACAC
	R	CGTGGTAGGTAAGGATCGCTG
TMEM158	F	CTGAACCGTAAGCCCATTGAG
	R	CGCTCCACACCACGATGAC
ODF3L1	F	AGGAGCCATTGCCCTCAAG
	R	GGCTATGCAGGGTATAAGCTG
SAA1	F	TCCCAACAAGATTATCATTTCC
	R	TGGCAGCATCATAGTTCC

F, forward; R, reversed.

Statistical analysis

Statistical analyses were performed using GraphPad Prism 8.0. Data are reported as the mean ± standard deviation. Student's *t*-test was used to assess differences between two groups and one-way analysis of variance (ANOVA) was used to assess differences between three or more groups. Differences were considered statistically significant at $p < 0.05$.

Results

Characterization of the prepared USPIO nanoparticles

Based on the results of Figure S1A and S1B (in Supplementary material), the particle sizes of USPIO-1, USPIO-2, and USPIO-3 were approximately 60 nm, and the zeta potential of USPIO-1, USPIO-2, and USPIO-3 were −32.9, −23.6, and
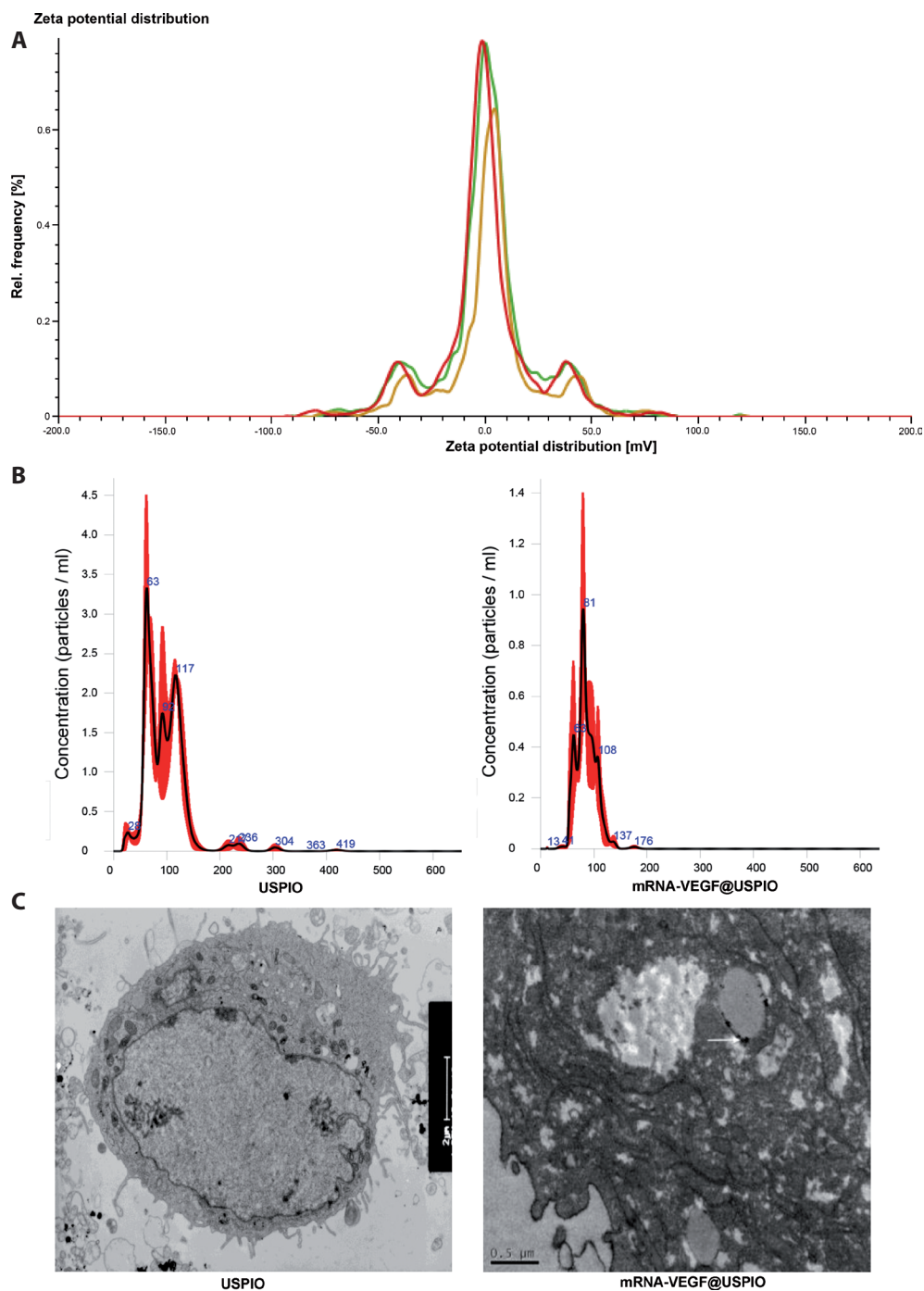
Figure 1. Identification of the constructed mRNA-VEGF@USPIO nanoparticles. **A.** The zeta potential of the mRNA-VEGF@USPIO nanoparticles. **B.** The particle size distributions of the USPIO and mRNA-VEGF@USPIO nanoparticles were determined by nanoparticle tracking analysis. **C.** The cellular uptake of the USPIO and mRNA-VEGF@USPIO nanoparticles by HBMECs using a transmission electron microscopy (TEM).
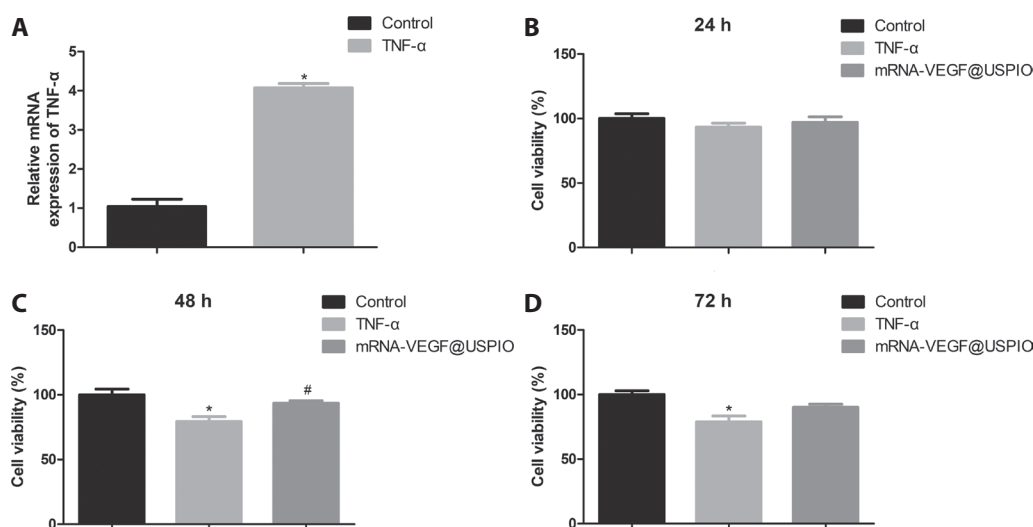
Figure 2. A. The expression level of TNF-α after HBMECs were induced by TNF-α. * $p < 0.05$ *vs.* control group ($n = 3$). Cell viability of HBMECs treated for 24 h (**B**), 48 h (**C**), and 72 h (**D**) using the CCK-8 assay. * $p < 0.05$ *vs.* control group; # $p < 0.05$ *vs.* TNF-α group ($n = 3$).

+3.7 mV, respectively. These results indicate that USPIO-1 has higher surface polymer content and is relatively stable. However, due to the addition of PEI, the overall potential of USPIO-3 was positive, and at the same time, due to the decrease in surface potential, the mutual repulsion force of the polymers on the surface of USPIO and the hydraulic size of the particles decreased.

TEM revealed that the particle sizes of USPIO-1 and USPIO-3 were similar, whereas the central particle size of USPIO-2 was larger (Fig. S2A). USPIO-1 and USPIO-3 were selected to investigate HBMEC uptake. Prussian blue staining showed that after co-culture, almost all the cells had a distinct blue color, and USPIO-3 displayed the strongest staining effect (Fig. S2B). ICP-OES results showed that the concentrations of Fe in the HBMECs after co-culturing with USPIO-1 and USPIO-3 were 23.8 ± 4.2 pg/cell and 161.2 ± 3.6 pg/cell, respectively. These results suggest that USPIO-1 and USPIO-3 could be taken up by HBMECs, and that HBMECs showed the strongest uptake capacity for USPIO-3.

Characterization of mRNA-VEGF@USPIO nanoparticles

Positively charged USPIO-3 was selected as the main probe and mRNA-VEGF@USPIO nanoparticles were constructed using a PEI-mediated method. After analyses, the concentration of mRNA VEGF in the mRNA-VEGF@USPIO nanocomposites detected was 50 ng/μl. The zeta potential of the mRNA-VEGF@USPIO nanoparticles was approximately −0.3 mV (favoring neutral, Fig. 1A). Additionally, NTA results showed that the primary particle

size peak of mRNA-VEGF@USPIO was 80.1 nm, which was larger than that of USPIO (62.4 nm) (Fig. 1B). TEM results showed that HBMECs could effectively take up both USPIO and mRNA-VEGF@USPIO. These results indicated that mRNA-VEGF@USPIO was successfully constructed and could be used for further experiments.

Effects of mRNA-VEGF@USPIO nanoparticles on the cell viability of HBMECs

HBMECs were treated with 10 ng/ml TNF-α for 24 h. A human brain microvascular endothelial cell injury model was constructed, and the expression of TNF-α was measured to evaluate the model. After TNF-α treatment, the expression of TNF-α was significantly upregulated compared with the control group ($p < 0.05$, Fig. 2A). These results suggest that human brain microvascular endothelial cell injury was successfully induced by TNF-α treatment.

Subsequently, the effects of the mRNA-VEGF@USPIO nanoparticles on the cell viability were explored. After co-culture for 24 h, there was no significant difference in cell viability between the control, TNF-α, and mRNA-VEGF@USPIO groups ($p > 0.05$, Fig. 2B). Whether co-cultured for 48 h or 72 h, cell viability of HBMECs was significantly inhibited after TNF-α treatment compared with the control group ($p < 0.05$, Fig. 2C and D), while there was no significant difference in cell viability between the mRNA-VEGF@USPIO group and the control group ($p > 0.05$, Fig. 2C and D). In addition, after co-culture for 48 h, mRNA-VEGF@USPIO nanoparticles significantly increased the cell viability of HBMECs compared with the TNF-α group ($p < 0.05$, Fig. 2C).

Transcriptome sequencing

Cells in the control, TNF-α, and mRNA-VEGF@USPIO groups were sequenced and DEGs between the three groups were analyzed. A total of 9063 DEGs were identified between the control and TNF-α groups, of which 4647 were upregulated and 4416 were downregulated (Fig. 3A). A total of 9125 DEGs were identified between the control and mRNA-VEGF@USPIO groups, including 4716 upregulated and 4409 downregulated DEGs (Fig. 3B). In addition, 211 DEGs were identified between the TNF-α and mRNA-VEGF@USPIO groups, including 179 upregulated DEGs and 32 downregulated DEGs (Fig. 3C). The heatmap distribution of DE-lncRNA expression is shown in Figure 3D. Overlapping DEGs were identified using Venn diagrams, and 71 overlapping DEGs were identified among the three groups (Fig. 3E).

These 71 overlapping DEGs were subjected to functional analyses. Figure 4 shows the top ten GO terms: including cellular component (CC), molecular function (MF), and biological process (BP), with extracellular space, extracellular region, cytokine activity, receptor ligand activity, response to lipopolysaccharides, and response to molecules of bacterial origin. KEGG analysis showed that these overlapping DEGs were mainly enriched in the IL-17 signaling pathway, Rheumatoid arthritis, Cytokine–cytokine receptor interaction, TNF signaling pathway, NF-κB signaling pathway, and NOD-like receptor signaling pathway.

RT-qPCR verification

Subsequently, eight overlapping DEGs were selected for validation using RT-qPCR. As shown in Figure 5, the expression levels of *PCDH1*, *ABCG4*, *SERPINA1*, *NDRG2*, *TMEM158*, *ODF3L1*, and *SAA1* were significantly downregulated in the TNF-α group, while the expression level of *RIMS1* was significantly up-regulated in the TNF-α group compared to the control group ($p < 0.05$, Fig. 5). Compared with TNF-α group, the expression levels of *PCDH1*, *ABCG4*, *SERPINA1*, *NDRG2*, *TMEM158*, *ODF3L1*, and *SAA1* were significantly increased, while the expression level of *RIMS1* was significantly decreased in the mRNA-VEGF@USPIO group ($p < 0.05$, Fig. 5). There were no significant differences in the expression levels of *PCDH1* or *ODF3L1* between the mRNA-VEGF@USPIO and control groups. The qPCR-based expression trends of these selected genes were in 87.5% agreement with the RNA-sequencing results, confirming the reliability and validity of the RNA-sequencing technique.

Discussion

Endothelial cells ensure normal vasoconstriction and diastole, and have specific functions, such as regulating blood pressure and maintaining the balance of coagulation and anticoagulation factors in the blood. Functional and structural integrity of the cerebral microvascular endothelium is essential for maintaining homeostasis in the cerebrovascular system. HBMEC injury can lead to the development of several cerebrovascular diseases (e.g., ischemic stroke and subarachnoid hemorrhage) (Abdullahi et al. 2018; Peeyush Kumar et al. 2019; Yan et al. 2020). Cerebrovascular diseases are a serious threat to human health with high rates of death and disability (Göthe et al. 2012). Therefore, measures should be taken to repair HBMEC injury when it occurs. In this study, we successfully constructed mRNA-VEGF@USPIO nanoparticles and used them to repair HBMEC injury. We found that the mRNA-VEGF@USPIO nanoparticles restored the decrease in cell viability caused by injury. Cells in the control, TNF-α, and mRNA-VEGF@USPIO groups were sequenced; 9063 DEGs were identified between the control and TNF-α groups, 9125 DEGs were identified between the control and mRNA-VEGF@USPIO groups, and 211 DEGs were identified between the TNF-α and mRNA-VEGF@USPIO groups. Overlapping DEGs were identified using Venn diagrams, and 71 overlapping DEGs were identified in these three groups. These 71 overlapping DEGs were related to the extracellular space, extracellular region, cytokine activity, receptor ligand activity, response to lipopolysaccharides, and response to molecules of bacterial origin. KEGG analysis showed that these overlapping DEGs were mainly enriched in cytokine-cytokine receptor interaction, the IL-17 signaling pathway, TNF signaling pathway, NF-κB signaling pathway, and NOD-like receptor signaling pathway. These results suggest that mRNA-VEGF@USPIO nanoparticles may be a novel approach for repairing HBMEC injuries.

HBMECs are the first neurovascular to sense hypoxic stimulation after cerebral ischemia injury, and their barrier function may be damaged and lead to vascular leakage (Page et al. 2016). VEGF is one of the most important proangiogenic factors in the choroidal angiogenic microenvironment. Numerous studies have confirmed that VEGF plays a key role in pathological neovascularization (Avraham et al. 2003; Silwedel et al. 2019). VEGF acts as a specific mitogen for endothelial cells, induces vascular endothelial cell division and proliferation, promotes endothelial cell migration, and facilitates new vessel outgrowth to form a large number of vessels (Greenberg and Jin 2005; Jin et al. 2020). USPIO is increasingly used as a small-molecule (5–40 nm diameter) magnetic nanoparticle for cell labeling because of its good biocompatibility and pluripotency (Avraham et al. 2003; Yang et al. 2011). In this study, the successful construction of mRNA-VEGF@USPIO nanoparticles was confirmed by NTA and spectrophotometry, and HBMECs were able to take up the mRNA-VEGF@USPIO nanoparticles. The CCK-8 results suggest that endothelial cell injury leads to a decrease in cell viability, and that the addition of mRNA-
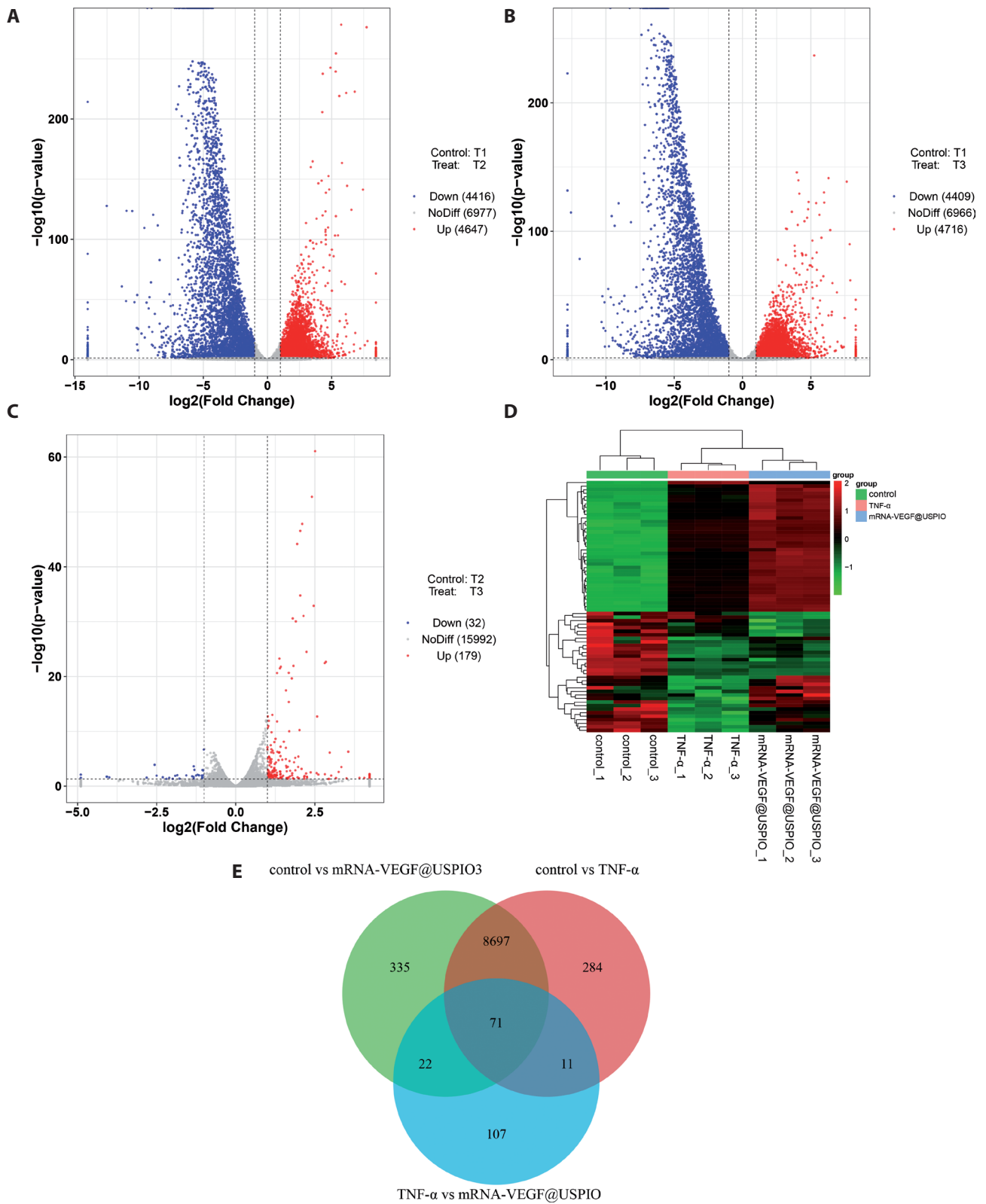
Figure 3. A. Volcano plot of DEGs between the control and TNF-α groups. **B.** Volcano plot of DEGs between the control and mRNA-VEGF@USPIO groups. **C.** Volcano plot of DEGs between the TNF-α and mRNA-VEGF@USPIO groups. **D.** Heat map of DEGs. **E.** Venn diagram of DEGs.
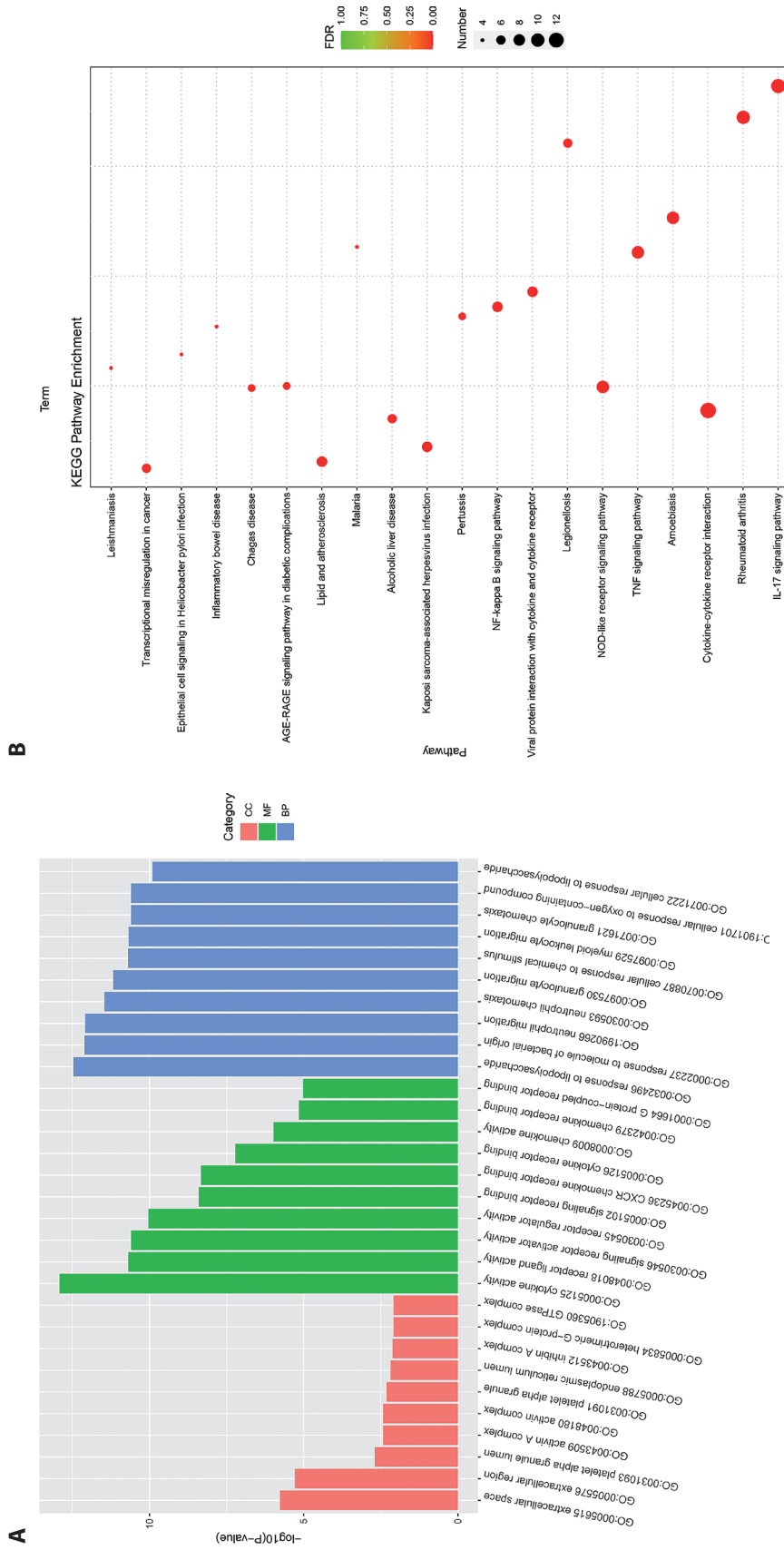
Figure 4. Functional analysis. **A.** Gene Ontology (GO) annotation of the predicted targets. **B.** Kyoto Encyclopedia of Genes and Genomes (KEGG) pathway enrichment analysis of the predicted targets.
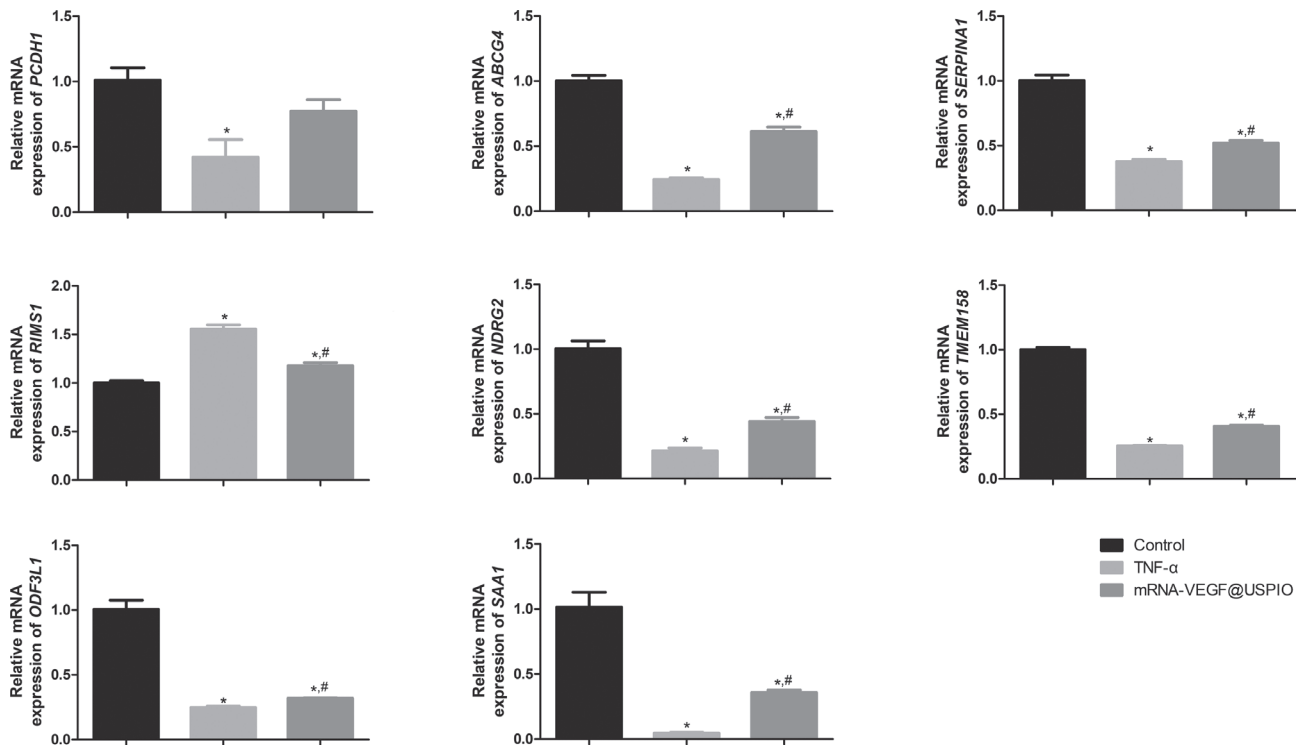
Figure 5. Expression of *PCDH1*, *ABCG4*, *SERPINA1*, *NDRG2*, *TMEM158*, *RIMS1, ODF3L1*, and *SAA1*. * $p < 0.05$, compared with the control group; # $p < 0.05$, compared with the TNF-α group.

VEGF@USPIO nanoparticles restores the changes in cell viability caused by the injury, suggesting that mRNA-VEGF@USPIO nanoparticles may be a new therapeutic modality for the treatment of endothelial cell injury. Nanoparticles have a cycle half-life that is closely related to their size and surface charge (Hoshyar et al. 2016). A previous study showed that nanoparticles smaller than approximately 10 nm in diameter are rapidly eliminated by the kidneys (Zuckerman et al. 2012). In addition, nanoparticles can enter cells *via* endocytosis, thereby regulating cell fate and initiating intercellular communication (Behzadi et al. 2017). The transport of nanomaterials into the cell ends with exocytosis, which may cause cytotoxicity (Sakhtianchi et al. 2013). However, the cytotoxicity of mRNA-VEGF@USPIO remains unclear and requires further exploration.

To further investigate the molecular mechanism of the mRNA-VEGF@USPIO nanoparticles, cells in the control, TNF-α, and mRNA-VEGF@USPIO groups were sequenced. This study identified 9063 DEGs between the control and TNF-α groups, 9125 DEGs between the control and mRNA-VEGF@USPIO groups, and 211 DEGs between the TNF-α and mRNA-VEGF@USPIO groups. Additionally, 71 overlapping DEGs were identified using Venn diagrams in these three groups. These overlapping DEGs were mainly enriched in cytokine-cytokine receptor interaction and the IL-17, TNF, NF-kappa B, and NOD-like receptor signaling pathways. A previous study showed that IL-17A plays an important role in neutrophil infiltration and neuronal damage following ischemia-reperfusion injury in the brain (Gelderblom et al. 2012). Moreover, several studies have demonstrated that targeting IL-17A-related signaling reduces acute inflammatory responses and tissue damage in cerebral ischemia (Nakae et al. 2002; Liao et al. 2012). Substantial evidence suggests that TNF-α plays a major role in initiating innate immune responses that involve triggering or amplifying local inflammatory responses (Wang et al. 2014; Chen et al. 2016). TNF-α has been reported to be a key cytokine in the inflammatory cascade response, triggering interactions between invading monocytes and vascular endothelial cells, and subsequently inducing apoptosis in circulating endothelial cells (Jia et al. 2015). Activation of NF-κB is essential for the production of circulating and local vascular TNF-α, as well as adhesion molecules, and leads to endothelial dysfunction in many pathophysiological conditions (Zhang et al. 2009). In summary, we speculated that mRNA-VEGF@USPIO nanoparticles may repair endothelial cell injury through cytokine-cytokine receptor interaction, the IL-17 signaling pathway, TNF signaling pathway, NF-κB signaling pathway, and NOD-like receptor signaling pathway.

Subsequently, the expression levels of *PCDH1*, *ABCG4*, *SERPINA1*, *NDRG2*, *TMEM158*, *RIMS1*, *ODF3L1*, and *SAA1* were verified using RT-qPCR. The results showed that the expression levels of *PCDH1*, *ABCG4*, *SERPINA1*, *NDRG2*, *TMEM158*, *ODF3L1*, and *SAA1* were significantly downregulated in the TNF-α group compared with the control group, while the expression level of *RIMS1* was significantly upregulated in the TNF-α group. Moreover, the expression levels of *PCDH1*, *ABCG4*, *SERPINA1*, *NDRG2*, *TMEM158*, *ODF3L1*, and *SAA1* were significantly increased in cells compared with the TNF-α group, while the expression level of *RIMS1* was significantly decreased in the mRNA-VEGF@USPIO group. *PCDH1* is a member of the δ-procalciferol subgroup of non-clustered procalciferol and is normally expressed in the brain, airway epithelium, skin keratin-forming cells and lungs (Bononi et al. 2008; Koning et al. 2012; Modak and Sotomayor 2019). *PCDH1* is localized to cell-cell contacts in epithelial cells, and *PCDH1* knockdown impairs epithelial barrier function (Faura Tellez et al. 2016). Knockdown of *PCDH1* in human cell lines and protoendothelial cells has been found to significantly reduce the susceptibility to a variety of New World viruses (Jangra et al. 2018). *ABCG4* is a member of the cholesterol transporter family that mediates cholesterol efflux and is expressed on the luminal membranes of cerebrovascular endothelial cells, neurons, and glial cells in the brain (Sano et al. 2016). *ABCG4* has been found to be involved in platelet differentiation and function, which is associated with the pathogenesis of cardiovascular disease (Schumacher and Benndorf 2017; Wang and Westerterp 2020). *SERPINA1* is a serine protease inhibitor that has been extensively studied in the fields of biochemistry and human diseases (DeMeo and Silverman 2004). *SERPINA1* expression is higher in patients with ischemic stroke than in controls (Liu et al. 2020). The *NDRG2* gene is a member of the NDRG family and is involved in the regulation of cell differentiation and spreading (Deng et al. 2003). *NDRG2* has been shown to be expressed in the embryonic ventricular zone, as well as in neurogenic regions of the adult brain, and *NDRG2* is associated with the blood-brain barrier (Jin et al. 2019; Zhu et al. 2020; Takarada-Iemata 2021). *SAA1* is an acute-phase protein that regulates inflammation and immunity (Lv et al. 2022). *SAA1* mediates leukocyte recruitment, angiogenesis, and matrix degradation in human microvascular endothelial cells (Dunk et al. 2012). In addition, increased *SAA1* levels are correlated with the severity of acute inflammation and injury (Gao et al. 2014). Based on these results, we hypothesized that these genes play important roles in HBMECs injury. However, the exact underlying mechanism requires further investigation.

In conclusion, mRNA-VEGF@USPIO nanoparticles can repair HBMECs injury. The possible molecular repair mechanism of the mRNA-VEGF@USPIO nanoparticles in HBMECs may be related to the expression of *PCDH1, ABCG4, SERPINA1, NDRG2, RIMS1, TMEM158, ODF3L1,* and *SAA1*. In addition, mRNA-VEGF@USPIO nanoparticles may be associated with the expression of mRNA-VEGF@USPIO nanoparticles through cytokine-cytokine receptor interaction, the IL-17 signaling pathway, TNF signaling pathway, NF-κB signaling pathway, and NOD-like receptor signaling pathway to repair HBMEC injury. Our results provide a theoretical basis for the application of mRNA-VEGF@USPIO nanoparticles for the treatment of HBMECs.

Author contributions. QZ conceived and designed and supervised the project. ZJ conducted the experiments. QZ and ZJ contributed to data analysis and manuscript drafting. All authors have read and approved the final version of the manuscript.

Reference

Abadie Y, Bregeon F, Papazian L, Lange F, Chailley-Heu B, Thomas P, Duveldestin P, Adnot S, Maitre B, Delclaux C (2005): Decreased VEGF concentration in lung tissue and vascular injury during ARDS. Eur. Respir. J. **25,** 139-146
https://doi.org/10.1183/09031936.04.00065504

Abdullahi W, Tripathi D, Ronaldson PT (2018): Blood-brain barrier dysfunction in ischemic stroke: targeting tight junctions and transporters for vascular protection. Am. J. Physiol. Cell Physiol. **315,** C343-356
https://doi.org/10.1152/ajpcell.00095.2018

Avraham HK, Lee TH, Koh Y, Kim TA, Jiang S, Sussman M, Samarel AM, Avraham S (2003): Vascular endothelial growth factor regulates focal adhesion assembly in human brain microvascular endothelial cells through activation of the focal adhesion kinase and related adhesion focal tyrosine kinase. J. Biol. Chem. **278,** 36661-36668
https://doi.org/10.1074/jbc.M301253200

Behzadi S, Serpooshan V, Tao W, Hamaly MA, Alkawareek MY, Dreaden EC, Brown D, Alkilany AM, Farokhzad OC, Mahmoudi M (2017): Cellular uptake of nanoparticles: journey inside the cell. Chem. Soc. Rev. **46,** 4218-4244
https://doi.org/10.1039/C6CS00636A

Bononi J, Cole A, Tewson P, Schumacher A, Bradley R (2008): Chicken protocadherin-1 functions to localize neural crest cells to the dorsal root ganglia during PNS formation. Mech. Dev. **125,** 1033-1047
https://doi.org/10.1016/j.mod.2008.07.007

Candelario-Jalil E (2009): Injury and repair mechanisms in ischemic stroke: considerations for the development of novel neurotherapeutics. Curr. Opin. Investig. Drugs **10,** 644-654

Catar R, Moll G, Hosp I, Simon, M, Luecht C, Zhao H, Wu D, Chen L, Kamhieh-Milz J, Korybalska K, et al. (2021): Transcriptional regulation of thrombin-induced endothelial VEGF induction and proangiogenic response. Cells **10,** 910
https://doi.org/10.3390/cells10040910

Chen PJ, Wang YL, Kuo LM, Lin CF, Chen CY, Tsai YF, Shen JJ, Hwang TL (2016): Honokiol suppresses TNF-α-induced neutrophil adhesion on cerebral endothelial cells by disrupting polyubiquitination and degradation of IκBα. Sci. Rep. **6,** 26554
https://doi.org/10.1038/srep26554

Corot C, Robert P, Idée JM, Port M (2006): Recent advances in iron oxide nanocrystal technology for medical imaging. Adv. Drug Deliv. Rev. **58,** 1471-1504
https://doi.org/10.1016/j.addr.2006.09.013

DeMeo DL, Silverman EK (2004): Alpha1-antitrypsin deficiency. 2: genetic aspects of alpha(1)-antitrypsin deficiency: phenotypes and genetic modifiers of emphysema risk. Thorax **59,** 259-264
https://doi.org/10.1136/thx.2003.006502

Deng W, Fan C, Shen R, Wu Y, Du R, Teng J (2020): Long noncoding MIAT acting as a ceRNA to sponge microRNA-204-5p to participate in cerebral microvascular endothelial cell injury after cerebral ischemia through regulating HMGB1. J. Cell. Physiol. **235,** 4571-4586
https://doi.org/10.1002/jcp.29334

Deng Y, Yao L, Chau L, Ng SS, Peng Y, Liu X, Au W, Wang J, Li F, Ji S, et al. (2003): N-Myc downstream-regulated gene 2 (NDRG2) inhibits glioblastoma cell proliferation. Int. J. Cancer **106,** 342-347
https://doi.org/10.1002/ijc.11228

Di Marco M, Sadun C, Port M, Guilbert I, Couvreur P, Dubernet C (2007): Physicochemical characterization of ultrasmall superparamagnetic iron oxide particles (USPIO) for biomedical application as MRI contrast agents. Int. J. Nanomedicine **2,** 609-622

Dunk CE, Roggensack AM, Cox B, Perkins JE, Åsenius F, Keating S, Weksberg R, Kingdom JCP, Adamson SL (2012): A distinct microvascular endothelial gene expression profile in severe IUGR placentas. Placenta **33,** 285-293
https://doi.org/10.1016/j.placenta.2011.12.020

Ediriweera GR, Chen L, Yerbury JJ, Thurecht KJ, Vine KL (2021): Non-viral vector-mediated gene therapy for ALS: challenges and future perspectives. Mol. Pharm. **18,** 2142-2160
https://doi.org/10.1021/acs.molpharmaceut.1c00297

Eichmann A, Simons M (2012): VEGF signaling inside vascular endothelial cells and beyond. Curr. Opin. Cell. Biol. **24,** 188-193
https://doi.org/10.1016/j.ceb.2012.02.002

El-Sayed Mohammed Youssef H, Eldeen Abo-Azma NE, Eldeen Megahed EM (2015): Correlation of hypoxia-inducible factor-1 alpha (HIF-1α) and vascular endothelial growth factor (VEGF) expressions with clinico-pathological features of oral squamous cell carcinoma (OSCC). Tanta. Dental. J. **12,** S1-S14
https://doi.org/10.1016/j.tdj.2015.05.010

Faura Tellez G, Willemse BW, Brouwer U, Nijboer-Brinksma S, Vandepoele K, Noordhoek JA, Heijink I, de Vries M, Smithers NP, Postma DS, et al. (2016): Protocadherin-1 localization and cell-adhesion function in airway epithelial cells in asthma. PLoS. One **11,** e0163967
https://doi.org/10.1371/journal.pone.0163967

Ferrara N (2009): VEGF-A: a critical regulator of blood vessel growth. Eur. Cytokine Netw. **20,** 158-163
https://doi.org/10.1684/ecn.2009.0170

Gao W, Lu C, Kochanek PM, Berger RP (2014): Serum amyloid A is increased in children with abusive head trauma: a gel-based proteomic analysis. Pediatr. Res. **76,** 280-286
https://doi.org/10.1038/pr.2014.86

Gelderblom M, Weymar A, Bernreuther C, Velden J, Arunachalam P, Steinbach K, Orthey E, Arumugam TV, Leypoldt F, Simova O, et al. (2012): Neutralization of the IL-17 axis diminishes neutrophil invasion and protects from ischemic stroke. Blood **120,** 3793-3802
https://doi.org/10.1182/blood-2012-02-412726

Göthe F, Enache D, Wahlund LO, Winblad B, Crisby M, Lökk J, Aarsland D (2012): Cerebrovascular diseases and depression: epidemiology, mechanisms and treatment. Panminerva. Med. **54,** 161-170

Greenberg DA, Jin K (2005): From angiogenesis to neuropathology. Nature **438,** 954-959
https://doi.org/10.1038/nature04481

Hoshyar N, Gray S, Han H, Bao G (2016): The effect of nanoparticle size on in vivo pharmacokinetics and cellular interaction. Nanomedicine (Lond) **11,** 673-692
https://doi.org/10.2217/nnm.16.5

Ikeda Y, Yonemitsu Y, Onimaru M, Nakano T, Miyazaki M, Kohno R, Nakagawa K, Ueno A, Sueishi K, Ishibashi T (2006): The regulation of vascular endothelial growth factors (VEGF-A, -C, and -D) expression in the retinal pigment epithelium. Exp. Eye Res. **83,** 1031-1040
https://doi.org/10.1016/j.exer.2006.05.007

Jangra RK, Herbert AS, Li R, Jae LT, Kleinfelter LM, Slough MM, Barker S, Guardado-Calvo P, Román-Sosa G, Dieterle ME, et al. (2018): Protocadherin-1 is essential for cell entry by New World hantaviruses. Nature **563,** 559-563
https://doi.org/10.1038/s41586-018-0702-1

Jia Z, Nallasamy P, Liu D, Shah H, Li JZ, Chitrakar R, Si H, McCormick J, Zhu H, Zhen W, et al. (2015). Luteolin protects against vascular inflammation in mice and TNF-alpha-induced monocyte adhesion to endothelial cells via suppressing IKBα/NF-κB signaling pathway. J. Nutr. Biochem. **26,** 293-302
https://doi.org/10.1016/j.jnutbio.2014.11.008

Jiang S, Zhao G, Lu J, Jiang M, Wu Z, Huang Y, Huang J, Shi J, Jin J, Xu X, et al. (2020). Silencing of circular RNA ANRIL attenuates oxygen-glucose deprivation and reoxygenation-induced injury in human brain microvascular endothelial cells by sponging miR-622. Biol. Res. **53,** 1-12
https://doi.org/10.1186/s40659-020-00295-2

Jin ML, Zou ZH, Tao T, Li J, Xu J, Luo KJ, Liu Z (2020): Effect of the recombinant adenovirus-mediated HIF-1 alpha on the expression of VEGF in the hypoxic brain microvascular endothelial cells of rats. Neuropsychiatr. Dis. Treat. **16,** 397-406
https://doi.org/10.2147/NDT.S238616

Jin PP, Xia F, Ma BF, Li Z, Zhang GF, Deng YC, Tu ZL, Zhang XX, Hou SX (2019): Spatiotemporal expression of NDRG2 in the human fetal brain. Ann. Anat. **221,** 148-155

https://doi.org/10.1016/j.aanat.2018.09.010

Katt ME, Xu ZS, Gerecht S, Searson PC (2016): Human brain microvascular endothelial cells derived from the BC1 iPS cell line exhibit a blood-brain barrier phenotype. PLoS One **11,** e0152105

https://doi.org/10.1371/journal.pone.0152105

Kay MA, Glorioso JC, Naldini L (2001): Viral vectors for gene therapy: the art of turning infectious agents into vehicles of therapeutics. Nat. Med. **7,** 33-40

https://doi.org/10.1038/83324

Kim M, Mok H, Yeo WS, Ahn JH, Choi YK (2021): Role of ginseng in the neurovascular unit of neuroinflammatory diseases focused on the blood-brain barrier. J. Ginseng Res. **45,** 599-609.

https://doi.org/10.1016/j.jgr.2021.02.003

Koning H, Sayers I, Stewart CE, de Jong D, Ten Hacken NH, Postma DS, van Oosterhout AJM, Nawijn MC, Koppelman GH (2012): Characterization of protocadherin-1 expression in primary bronchial epithelial cells: association with epithelial cell differentiation. FASEB J. **26,** 439-448

https://doi.org/10.1096/fj.11-185207

Liao YH, Xia N, Zhou SF, Tang TT, Yan XX, Lv BJ, Nie SF, Wang J, Iwakura Y, Xiao H, et al. (2012): Interleukin-17A contributes to myocardial ischemia/reperfusion injury by regulating cardiomyocyte apoptosis and neutrophil infiltration. J. Am. Coll. Cardiol. **59,** 420-429

https://doi.org/10.1016/j.jacc.2011.10.863

Liu Q, Cui P, Zheng K, Wang J, Jiang W, Liu G, Hao J, Liu H (2020): SERPINA1 gene expression in whole blood links the rs6647 variant G allele to an increased risk of large artery atherosclerotic stroke. FASEB J. **34,** 10107-10116

https://doi.org/10.1096/fj.201903197R

Lv Z, Duan S, Zhou M, Gu M, Li S, Wang Y, Xia Q, Xu D, Mao Y, Dong W, et al. (2022): Mouse bone marrow mesenchymal stem cells inhibit sepsis-induced lung injury in mice via exosomal SAA1. Mol. Pharm. **19,** 4254-4263

https://doi.org/10.1021/acs.molpharmaceut.2c00542

Mammen B, Ramakrishnan T, Sudhakar U (2007): Principles of gene therapy. Indian J. Dent. Res. **18,** 196

https://doi.org/10.4103/0970-9290.35832

Modak D, Sotomayor M (2019): Identification of an adhesive interface for the non-clustered δ1 protocadherin-1 involved in respiratory diseases. Commun. Biol. **2,** 354

https://doi.org/10.1038/s42003-019-0586-0

Nag S, Eskandarian MR, Davis J, Eubanks JH (2002): Differential expression of vascular endothelial growth factor-A (VEGF-A) and VEGF-B after brain injury. J. Neuropathol. Exp. Neurol. **61,** 778-788

https://doi.org/10.1093/jnen/61.9.778

Nakae S, Komiyama Y, Nambu A, Sudo K, Iwase M, Homma I, Sekikawa K, Asano M, Iwakura Y (2002): Antigen-specific T cell sensitization is impaired in IL-17-deficient mice, causing suppression of allergic cellular and humoral responses. Immunity **17,** 375-387

https://doi.org/10.1016/S1074-7613(02)00391-6

O'Connor BB, Grevesse T, Zimmerman JF, Ardoña HAM, Jimenez JA, Bitounis D, Demokritou P, Parker KK (2020): Human brain microvascular endothelial cell pairs model tissue-level blood-brain barrier function. Integr. Biol. (Camb) **12,** 64-79

https://doi.org/10.1093/intbio/zyaa005

Page S, Munsell A, Al-Ahmad AJ (2016): Cerebral hypoxia/ischemia selectively disrupts tight junctions complexes in stem cell-derived human brain microvascular endothelial cells. Fluids Barriers CNS **13,** 16

https://doi.org/10.1186/s12987-016-0042-1

Peeyush Kumar T, McBride DW, Dash PK, Matsumura K, Rubi A, Blackburn SL (2019): Endothelial cell dysfunction and injury in subarachnoid hemorrhage. Mol. Neurobiol. **56,** 1992-2006

https://doi.org/10.1007/s12035-018-1213-7

Richard S, Eder V, Caputo G, Journé C, Ou P, Bolley J, Louedec L, Guenin E, Motte L, Pinna N, et al. (2016): USPIO size control through microwave nonaqueous sol-gel method for neoangiogenesis T2 MRI contrast agent. Nanomedicine (Lond) **11,** 2769-2779

https://doi.org/10.2217/nnm-2016-0177

Rui YP, Liang B, Hu F, Xu J, Peng YF, Yin PH, Duan YR, Zhang CF, Gu HC (2016): Ultra-large-scale production of ultrasmall superparamagnetic iron oxide nanoparticles for T1-weighted MRI. J. RSC Advances **6,** 22575-22585

https://doi.org/10.1039/C6RA00347H

Sakhtianchi R, Minchin RF, Lee KB, Alkilany AM, Serpooshan V, Mahmoudi M (2013): Exocytosis of nanoparticles from cells: role in cellular retention and toxicity. Adv. Colloid. Interface Sci. 201-202, 18-29

https://doi.org/10.1016/j.cis.2013.10.013

Sano O, Tsujita M, Shimizu Y, Kato R, Kobayashi A, Kioka N, Remaley AT, Michikawa M, Ueda K, Matsuo M (2016): ABCG1 and ABCG4 suppress γ-secretase activity and amyloid β production. PLoS One **11,** e0155400

https://doi.org/10.1371/journal.pone.0155400

Schumacher T, Benndorf RA (2017): ABC transport proteins in cardiovascular disease-a brief summary. Molecules **22,** 589

https://doi.org/10.3390/molecules22040589

Schütz CA, Staedler D, Crosbie-Staunton K, Movia D, Bernasconi CC, Kenzaoui BH, Prina-Mello A, Juillerat-Jeanneret L (2014): Differential stress reaction of human colon cells to oleic-acid-stabilized and unstabilized ultrasmall iron oxide nanoparticles. Int. J. Nanomedicine **9,** 3481-3498

https://doi.org/10.2147/IJN.S65082

Shakil MS, Hasan M, Sarker SR (2019): Iron oxide nanoparticles for breast cancer theranostics. Curr. Drug Metab. **20,** 446-456

https://doi.org/10.2174/1389200220666181122105043

Silwedel C, Speer CP, Haarmann A, Fehrholz M, Claus H, Schlegel N, Glase K (2019): Ureaplasma species modulate cell adhesion molecules and growth factors in human brain microvascular endothelial cells. Cytokine **121,** 154737

https://doi.org/10.1016/j.cyto.2019.154737

Sun NF, Liu ZA., Huang WB, Tian AL, Hu SY (2014): The research of nanoparticles as gene vector for tumor gene therapy. Crit. Rev. Oncol. Hematol. **89,** 352-357

https://doi.org/10.1016/j.critrevonc.2013.10.006

Takarada-Iemata M (2021): Roles of N-myc downstream-regulated gene 2 in the central nervous system: molecular basis and relevance to pathophysiology. Anat. Sci. Int. **96,** 1-12

https://doi.org/10.1007/s12565-020-00587-3

Wang N, Westerterp M (2020): ABC transporters, cholesterol efflux, and implications for cardiovascular diseases. Adv. Exp. Med. Biol. **1276,** 67-83
https://doi.org/10.1007/978-981-15-6082-8_6

Wang Y, Li Y, Wu Y, Jia L, Wang J, Xie B, Hui M, Du J (2014): 5TNF-α and IL-1β neutralization ameliorates angiotensin II-induced cardiac damage in male mice. Endocrinology **155,** 2677-2687
https://doi.org/10.1210/en.2013-2065

Yan G, Zhao H, Hong X (2020): LncRNA MACC1-AS1 attenuates microvascular endothelial cell injury and promotes angiogenesis under hypoxic conditions via modulating miR-6867-5p/TWIST1 in human brain microvascular endothelial cells. Ann. Transl. Med. **8,** 876
https://doi.org/10.21037/atm-20-4915

Yang J, Zaim Wadghiri Y, Minh Hoang D, Tsui W, Sun Y, Chung E, Li Y, Wang A, de Leon M, Wisniewski T (2011): Detection of amyloid plaques targeted by USPIO-Aβ1-42 in Alzheimer's disease transgenic mice using magnetic resonance microimaging. NeuroImage **55,** 1600-1609
https://doi.org/10.1016/j.neuroimage.2011.01.023

Li Y, Chen Z, Zhao Z, Li H, Wang J, Zhang Z (2012): The preparation of MR specific USPIO probes using one-pot method. J. Adv. Sci. Lett. **18,** 189-194
https://doi.org/10.1166/asl.2012.3687

Zhang H, Park Y, Wu J, Chen X, Lee S, Yang J, Dellsperger KC, Zhang C (2009): Role of TNF-alpha in vascular dysfunction. Clin. Sci. (Lond) **116,** 219-230
https://doi.org/10.1042/CS20080196

Zhu J, Yang LK, Wang QH, Lin W, Feng Y, Xu YP, Chen WL, Xiong K, Wang YH (2020): NDRG2 attenuates ischemia-induced astrocyte necroptosis via the repression of RIPK1. Mol. Med. Rep. **22,** 3103-3110
https://doi.org/10.3892/mmr.2020.11421

Zuckerman JE, Choi CH, Han H, Davis ME (2012): Polycation-siRNA nanoparticles can disassemble at the kidney glomerular basement membrane. Proc. Natl. Acad. Sci. USA **109,** 3137-3142
https://doi.org/10.1073/pnas.1200718109